International Journal of Solids and Structures 49 (2012) 1864–1876

Contents lists available at SciVerse ScienceDirect

International Journal of Solids and Structures

journal homepage: www.elsevier.com/locate/ijsolstr

# Symmetry breaking in an initially curved micro beam loaded by a distributed electrostatic force

Lior Medina [a,*], Rivka Gilat [b], Slava Krylov [a]

[a] Faculty of Engineering, School of Mechanical Engineering, Tel Aviv University, Ramat Aviv 69978, Israel
[b] Department of Civil Engineering, Faculty of Engineering, Ariel University Center, Ariel 44837, Israel

ARTICLE INFO

*Article history:*
Received 28 October 2011
Received in revised form 19 March 2012
Available online 5 April 2012

*Keywords:*
Curved micro beam
Electrostatic force
Bistability
Snap-through buckling
MEMS/NEMS
Elastic foundation
Non-symmetric buckling criteria

ABSTRACT

The asymmetric buckling of a shallow initially curved stress-free micro beam subjected to distributed nonlinear deflection-dependent electrostatic force is studied. In order to highlight the symmetry breaking phenomenon and the approach to its analysis, the subsidiary simplified problem of a curved beam attached to a linearly elastic foundation, and subjected to uniformly distributed "mechanical" load, which is independent of deflections, is addressed first. The analysis is based on a two degrees of freedom reduced order (RO) model resulting from the Galerkin decomposition with linear undamped eigenmodes of a straight beam used as the base functions. Simple approximate expressions are derived defining the geometric parameters of beams for which an asymmetric response bifurcates from the symmetric one. The necessary criterion establishes the conditions for the appearance of bifurcation points on the unstable branch of the symmetric limit point buckling curve; the sufficient criterion assures a realistic asymmetric buckling bifurcating from the stable branches of the curve. It is shown that while the symmetry breaking conditions are affected by the nonlinearity of the electrostatic force, its influence is less pronounced than in the case of the symmetric snap-through criterion. A comparison between the RO model results and those obtained by direct numerical analysis shows good agreement between the two and indicates that the obtained criteria can be used to predict non-symmetric buckling in electrostatically actuated bistable micro beams.



## 1. Introduction

Initially curved beams (arches) loaded by concentrated or distributed transverse forces may exhibit bistability, namely, the existence of two different stable equilibria under the same loading. The transition between two stable states in these structures is commonly referred to as a snap-through buckling. The behavior of beams liable to the snap-through buckling is well understood and it is an established topic in structural mechanics (e.g., see Bažant and Cedolin, 1991; Dym, 1974; Seyranian and Elishakoff, 1989; Thompson and Hunt, 1973; Simitses, 1989; Timoshenko, 1961 and references therein. See Chen and Chang (2007), Mallon et al. (2006), Plaut (2009) and Plaut and Virgin (2009) for some of the recent contributions). On the most basic level, initially straight or slightly curved beams do not buckle under a transverse force, whereas sufficiently curved beams manifest a symmetric (limit point) snap-through and are bistable in the interval of the force between the snap-back (release) and snap-through values. When the initial curvature of the beam is higher than a certain value, the buckling is accompanied by a symmetry breaking and the appearance of non-symmetric buckling configurations.

Recently, a renewed interest in the mechanics of bistable beams stimulated additional studies (Das and Batra, 2009a,b; Krylov et al., 2008, 2011; Ouakad and Younis, 2010; Park and Hah, 2008; Pane and Asano, 2008; Saif, 2000; Qiu et al., 2004; Zhang et al., 2007) that were motivated by the progress in fabrication technologies and by the emerging of new applications in the realm of micro and nanoelectromechanical systems (MEMS and NEMS). The reason for this interest is twofold. On the one hand, micro and nano devices incorporating bistable structural elements have clear functional advantages in applications such as switches (Intaraprasonk and Fan, 2011), sensors (Southworth et al., 2010) and non-volatile memories (Charlot et al., 2008). On the other hand, over the past decade, electrostatically actuated initially straight double-clamped micro beam became a kind of benchmark problem, which was intensively used for the evaluation of various analytical, numerical and experimental approaches (see reviews Batra et al., 2007b; Nayfeh et al., 2003; Rhoads et al., 2008 and references therein). One of the distinguishing features of such a micro device is that it is loaded by an electrostatic force, which is a nonlinear function of the beam's deflections. For this reason, while being a relatively simple structure, a micro beam exhibits rich behavior and

* Corresponding author.
*E-mail address:* liormedi@post.tau.ac.il (L. Medina).

0020-7683/$ - see front matter © 2012 Elsevier Ltd. All rights reserved.
http://dx.doi.org/10.1016/j.ijsolstr.2012.03.040

represents a convenient platform for analytical, numerical and experimental investigation of the abundant nonlinear phenomena at the microscale, which are rarely encountered or are difficult to envisage within large scale structures. As an example of this kind of phenomena, one can mention electrostatic (so-called pull-in) instability taking place in micro beams and associated with the softening nonlinearity of the electrostatic forces, which reduces the effective stiffness of the structure.[1]

In contrast to straight beams, initially curved electrostatically actuated double-clamped beams combine both geometric mechanical nonlinearity typical for bistable structures and generic electrostatic softening nonlinearity. As was recently shown by Das and Batra (2009a), Das and Batra (2009b), Krylov et al. (2008) and Zhang et al. (2007), these structures may exhibit sequential snap-through buckling and pull-in instability. Note that the limit point snap-through and the symmetry breaking criteria for beams subjected to a "mechanical" deflection-independent loading are fully dictated by the geometry of the beam itself-namely by the ratio between the initial elevation/curvature of the beam and its thickness – and is independent on the loading (Dym, 1974; Simitses, 1989). However, in the case of the electrostatic actuation, the snap-through behavior is affected by the nonlinearity of the electrostatic force parameterized by the initial distance between the beam and the electrode, as reflected in the symmetric (limit-point) snap-through criterion first obtained in Krylov et al. (2008) for an initially stress-free bell-shaped beam. It was shown, that in the case of the electrostatic loading, the snap-through may take place in beams with lower initial elevation/curvature when compared to the case of "mechanical" deflection-independent loading.

It should be noted, that while relatively a large body of work was devoted to the stability and dynamics of straight and curved micro beams, the number of studies dealing with the non-symmetric buckling of these structures loaded by configuration-dependent electrostatic forces is limited. Non-symmetric buckling of curved bell-shaped beams subjected to distributed electrostatic loading was illustrated in Krylov et al. (2011) by means of the reduced-order and computational models. Symmetry breaking in a similar structure was analyzed in more details in Das and Batra (2009b) and was found to have significant influence on the stability boundaries of the beam: the snap-through voltage was shown to be lower than predicted by the symmetric model. Initially straight micro beams buckled due to pre-stress and then actuated by electrostatic force engendered by the fringing fields were analyzed numerically in Krylov et al. (2011) and were shown to exhibit non-symmetric buckling for sufficiently high values of the initial pre-stress and consequently curvature. Non-symmetric pull-in configurations of initially flat annular membranes were considered in Batra et al. (2007a) and Pelesko et al. (2003), non-symmetric pull-in configurations of annular plates under electrostatic and Casimir forces were obtained numerically in Batra et al. (2006). However, no symmetry-breaking criteria were obtained in all these works.

In this work, we extend the stability analysis of electrostatically actuated initially curved stress-free micro beams to the non-symmetric configurations. Our goal is to highlight the leading phenomena taking place in this type of structure, to investigate the influence of the device parameters on its stability and to establish criteria of symmetry breaking. We develop simple approximate relations between the geometrical parameters of the structure (thickness, initial elevation and distance between the beam and the electrode), which should be satisfied in order to obtain the non-symmetric buckling and find the values of the beam's deflection and of the actuation voltage corresponding to the critical points. These criteria are in a sense an extension of the well-documented results obtained for mechanically loaded curved beams (see Dym, 1974 and Simitses, 1989) to the case of the intrinsic nonlinear electrostatic loading.

In the next section, the problem of an initially curved bell-shaped stress-free beam under a distributed electrostatic force is formulated, followed by the development of a reduced order (RO) model based on the Galerkin decomposition and limited to incorporate two-symmetric and non-symmetric-terms. Next, an auxiliary problem of a curved beam resting on a linear (i.e, constant, deflection-independent, stiffness) elastic foundation and loaded by a "mechanical" force, which is independent on deflections, is considered and snap-through and symmetry breaking criteria are obtained. Due to its simplicity, this problem represents a convenient framework allowing simple closed form expressions. Then, the two-mode RO model of the electrostatically loaded beam is considered and the stability criteria are obtained along with the critical values of the deflections and actuation voltages. In the last section, the approximate results are verified using the numerical solution of the governing equations of the beam. Main findings of the work are summarized in the conclusions.

## 2. Formulation

We consider a flexible initially curved double clamped prismatic micro beam of length $L$ having a rectangular cross-section of width $\hat{b}$ and thickness $\hat{d}$ as shown in Fig. 1. The beam is made of homogeneous isotropic linearly elastic material with Young's modulus $E$. Since the width $\hat{b}$ of a microbeam is typically larger than it's thickness $\hat{d}$, an effective (plain strain) modulus of elasticity $\widetilde{E} = E/(1-\nu^2)$ is used, where $\nu$ is Poisson's ratio. The initial shape of the beam is described by the function $\hat{w}_0(\hat{x}) = \hat{h} z_0(\hat{x})$, where $\hat{h}$ is the initial elevation of the beam's central point above it's ends, and $z_0(\hat{x})$ is a non dimensional function such that $\max_{\hat{x}\in[0,L]}[z_0(\hat{x})] = 1$. The beam is subjected to a distributed electrostatic force provided by an electrode located at a distance $\hat{g}_0$ (the gap) from the beam and extended beyond it's ends.

We assume that $\hat{d} \ll L$, $\hat{h} \ll L$ and that the deflections, while comparable with the thickness of the beam, are small with respect to the beam's length. Under these assumptions, the beam's behavior is described in the framework of the Euler–Bernoulli theory combined with the shallow arch approximation and is governed by the following equilibrium equations (Simitses and Hodges, 2006; Villagio, 1997).

$$\widetilde{E}A\frac{\partial}{\partial\hat{x}}\left(\frac{\partial\hat{u}}{\partial\hat{x}}+\frac{1}{2}\left(\frac{\partial\hat{w}}{\partial\hat{x}}\right)^2-\frac{1}{2}\left(\frac{\partial\hat{w}_0}{\partial\hat{x}}\right)^2\right)=0 \tag{1}$$

$$\widetilde{E}I_{yy}\left(\frac{\partial^4\hat{w}}{\partial\hat{x}^4}-\frac{\partial^4\hat{w}_0}{\partial\hat{x}^4}\right)-\widetilde{E}A\left(\frac{\partial\hat{u}}{\partial\hat{x}}+\frac{1}{2}\left(\frac{\partial\hat{w}}{\partial\hat{x}}\right)^2-\frac{1}{2}\left(\frac{\partial\hat{w}_0}{\partial\hat{x}}\right)^2\right)\frac{\partial^2\hat{w}}{\partial\hat{x}^2}=\hat{f}^e \tag{2}$$

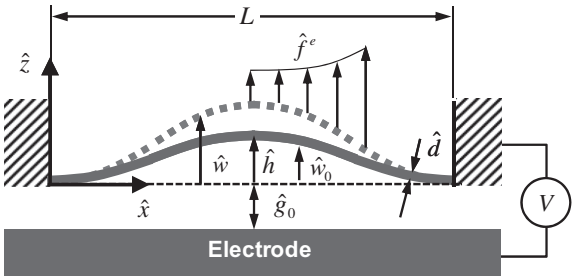


**Fig. 1.** Model of an initially curved double-clamped beam actuated by distributed electrostatic force. The dashed line corresponds to the deformed configuration. Positive directions of the beam's deflection and of the loading are shown.

[1] In large scale structures, the voltage required to initiate this instability is much larger than the electric breakdown voltage, the influence of the electrostatic force on the structure's deflection is not pronounced and the mechanical end electrostatic problems are decoupled.

with the homogeneous boundary conditions

$$\hat{u}(0)=\hat{u}(L)=0 \qquad \hat{w}(0)=\hat{w}(L)=0 \qquad \frac{\partial\hat{w}}{\partial\hat{x}}(0)=\frac{\partial\hat{w}}{\partial\hat{x}}(L)=0 \tag{3}$$

Here $A=\hat{b}\hat{d}$ and $I_{yy}=\hat{b}\hat{d}^3/12$, are the cross-section's area and the second moment of area, respectively; $\hat{w}(\hat{x})$ denotes the elevation of beam's axis above it's supports and $\hat{u}(\hat{x})$ represents the axial displacement of the beam. In addition, $\hat{f}^e$ is the applied electrostatic load, approximated by the parallel capacitor formula (note that the sign is taken to be consistent with Fig. 1).

$$\hat{f}^e=-\frac{\epsilon_0\hat{b}V^2}{2(\hat{g}_0+\hat{w})^2} \tag{4}$$

Here $\epsilon_0=8.854$ F/m is the permittivity of the free space and $V$ is the voltage difference between the beam and the electrode. Note that while the influence of the fringing fields on the electrostatic force acting on the curved beam could be taken into considerations (e.g., Das and Batra, 2009b), we use Eq. (4) for the sake of simplicity and transparency of the development.

In accordance with Eq. (1), the axial force is constant along the beam, hence Eqs. (1) and (2) can be reduced to the following single equation (e.g., Simitses and Hodges, 2006; Villagio, 1997)

$$\widetilde{E}I_{yy}\left(\frac{\partial^4\hat{w}}{\partial\hat{x}^4}-\frac{\partial^4\hat{w}_0}{\partial\hat{x}^4}\right)-\frac{\widetilde{E}A}{2L}\int_0^L\left(\left(\frac{\partial\hat{w}}{\partial\hat{x}}\right)^2-\left(\frac{\partial\hat{w}_0}{\partial\hat{x}}\right)^2\right)d\hat{x}\frac{\partial^2\hat{w}}{\partial\hat{x}^2}=\hat{f}^e \tag{5}$$

which is still subjected to the boundary conditions given by the last two of Eq. (3). In essence, the integral term in Eq. (5) represents the average of the axial force.

For convenience, we re-write Eqs. (1) and (2) in a non-dimensional form

$$\left(u'+\frac{1}{2}(w')^2-\frac{1}{2}(w_0')^2\right)'=0 \tag{6}$$

$$w^{IV}-w_0^{IV}-2\alpha\left(u'+\frac{1}{2}(w')^2-\frac{1}{2}(w_0')^2\right)w''=-\frac{\beta}{(1+w)^2} \tag{7}$$

where $()'$ denotes derivative with respect to the non-dimensional coordinate $0\leqslant x\leqslant 1$. The non-dimensional counterpart of Eq. (5) is

$$w^{IV}-w_0^{IV}-\alpha\int_0^1\left((w')^2-(w_0')^2\right)dx\,w''=-\frac{\beta}{(1+w)^2} \tag{8}$$

The non-dimensional quantities used in Eqs. (6)–(8) are defined in Table 1.

## 3. Reduced order model

In order to analyze the snap-through and pull-in behavior of the beam, a reduced order (RO) model based on the Galerkin decomposition is constructed. The deformed shape of the beam is approximated by the series

$$w(x)\approx\sum_{i=1}^{n}q_i\varphi_i(x) \tag{9}$$

where $q_i$ are the generalized coordinates, and $\varphi_i$ are the linear undamped eigenmodes of a straight stress free double-clamped beam and are given by the expression

$$\varphi_i(x)=C_i(J_i(\cos(\lambda_i x)-\cosh(\lambda_i x))+\sin(\lambda_i x)-\sinh(\lambda_i x)) \tag{10}$$

Here $J_i=(\cos\lambda_i-\cosh\lambda_i)/(\sinh\lambda_i+\sin\lambda_i)$; $C_i$ are constants, which are chosen such that $\max_{x\in[0,1]}(\varphi_i(x))=1$; $\lambda_i=(\omega_i)^{1/2}(\rho AL^4/EI)^{1/4}$ are the frequency parameters, which are related to the eigenfrequencies $\omega_i$ of the beam, and are found as solution's to the frequency equation $\cos\lambda_i\cosh\lambda_i=1$.

While beams of different initial shapes can be analyzed, we consider a beam of an initial shape that can be represented by the series

$$w_0(x)=\sum_{i=1}^{n}q_{0i}\varphi_i(x) \tag{11}$$

Substitution of Eqs. (9) and (11) into Eq. (8), multiplication by $\varphi_j$ and integration in conjunction with the orthogonality of the eigenmodes, produce a system of coupled nonlinear algebraic equations (see Krylov et al., 2011)

$$\mathbf{B}(\mathbf{q}-\mathbf{q}_0)+\alpha(\mathbf{q}^{\mathbf{T}}\mathbf{S}\mathbf{q}-\mathbf{q}_0^{\mathbf{T}}\mathbf{S}\mathbf{q}_0)\mathbf{S}\mathbf{q}=-\beta\mathbf{Q} \tag{12}$$

where $()^T$ denotes the matrix transpose, $\mathbf{q}=\{q_i\}$ and $\mathbf{q_0}=\{q_{0i}\}$. The elements of the generalized force vector $\mathbf{Q}=\{Q_i\}$ and of the matrices $\mathbf{B}=\{b_{ij}\}$ and $\mathbf{S}=\{s_{ij}\}$, which are associated with the bending and stretching stiffness of the beam, respectively, are given by

$$Q_i=\int_0^1\frac{\varphi_i}{\left(1+\sum_{j=1}^{n}q_j\varphi_j(x)\right)^2}dx \tag{13}$$

$$b_{ij}=\delta_{ij}\int_0^1\varphi_i''\varphi_j''dx\quad s_{ij}=\int_0^1\varphi_i'\varphi_j'dx \tag{14}$$

with $\delta_{ij}$ being the Kronecker delta. Note, that since $w(x)$ defines the shape (the elevation) of the beam rather than it's displacement (see Fig. 1), we have $-1\leqslant q_i$.

For the investigation of the asymmetric snap-through, the RO model should include at least two terms, the first symmetric and the first anti-symmetric ones. By setting $n=2$ in Eq. (9), and by using the initial shape corresponding to the fundamental mode of the straight beam, (i.e. Eq. (11) with $n=1$ and $q_{01}=h$), the RO model in Eq. (12) is reduced to the form of two coupled nonlinear algebraic equations in terms of the general coordinates $q_1$ and $q_2$

$$b_{11}(q_1-h)+\alpha s_{11}^2\left(q_1^2-h^2\right)q_1+\alpha s_{11}s_{22}q_2^2q_1=-\beta\int_0^1\frac{\varphi_1}{(1+q_1\varphi_1+q_2\varphi_2)^2}dx \tag{15}$$

$$b_{22}q_2+\alpha s_{11}s_{22}\left(q_1^2-h^2\right)q_2+\alpha s_{22}^2q_2^3=-\beta\int_0^1\frac{\varphi_2}{(1+q_1\varphi_1+q_2\varphi_2)^2}dx \tag{16}$$

where $b_{11}=198.463$, $b_{22}=1669.859$, $s_{11}=4.878$ and $s_{22}=20.218$. Note that taking the initial shape of the beam to have the form of the symmetric first mode with no imperfection, enables the capture of the symmetry breaking bifurcation points.

Due to the presence of the integral terms, which are associated with the electrostatic force, Eqs. (15) and (16) cannot be solved in a closed form. Note that, as typical in electrostatic MEMS, the deflection-dependent distributed electrostatic force affects the effective

**Table 1**
Non-dimensional quantities.

| | |
|---|---|
| $x\triangleq\hat{x}/L$ | Coordinate |
| $w\triangleq\hat{w}/\hat{g}_0,\ w_0\triangleq\hat{w}_0/\hat{g}_0$ | Elevation/initial elevation |
| $h\triangleq\hat{h}/\hat{g}_0$ | Initial midpoint elevation |
| $d\triangleq\hat{d}/\hat{g}_0$ | Thickness |
| $\alpha\triangleq(\hat{g}_0^2A)/(2I_{yy})$ | Stretching parameter |
| $\beta\triangleq(\epsilon_0\hat{b}V^2L^4)/(2\hat{g}_0^3\widetilde{E}I_{yy})$ | Voltage parameter |

stiffness of the system, and can be viewed in a sense as an elastic foundation with a nonlinear negative stiffness parameterized by voltage (e.g. see Elata and Abu-Salih, 2006; Krylov, 2008). In order to highlight ideas beyond the approach used for the symmetry breaking analysis of the electrostatically actuated curved beam and to illustrate the role of the electrostatic force in the snap-thorough behavior, we first consider a "mechanical" problem of a curved beam on an elastic foundation with a constant, independent on the deflections, stiffness. The beam is loaded by a uniformly distributed, prescribed, deflection-independent force. Note that while the stability analysis of such a beam was reported by several authors (e.g., see Simitses and Hodges, 2006 where a beam of a sinusoidal initial shape was considered), it is presented here in a general form, for both positive and negative foundations, for the sake of completeness. In addition, the snap-through and symmetry-breaking criteria derived in the next section provide an insight into the results obtained for the case of the electrostatic loading.

## 4. The case of deflection-independent loading and linearly elastic foundation

### 4.1. Reduced order model

We consider an initially curved double-clamped beam on a linearly elastic foundation of a constant stiffness $\hat{k}$, loaded by a uniformly distributed deflection-independent force $\hat{f}^M$ (acting in the negative direction of the $z$ axis, in accordance with Fig. 1). The equilibrium of the beam is described by the equation

$$w^{IV} - w_0^{IV} - \alpha \int_0^1 ((w')^2 - (w_0')^2)dx w'' + \gamma(w - w_0) = -\beta^M \tag{17}$$

where the non-dimensional stiffness parameter, $\gamma$, and the force parameter, $\beta^M$, are defined by the expressions

$$\gamma = \frac{\hat{k}L^4}{\widetilde{EI}_{yy}} \quad \beta^M = \frac{\hat{f}^M L^4}{\widetilde{EI}_{yy}\hat{g}_0} \tag{18}$$

and $\alpha$ is specified in Table 1. Here $\hat{g}_0$, which is preserved for the consistency with the formulation of the electrostatic problem, is taken to be an arbitrary unit of length. Note that $\gamma$ reflects the relative stiffness of the foundation with respect to the bending stiffness of the beam. As the uniform force $\beta$ in the right hand side of Eq. (17) is deflection-independent, and the integral is independent on the spatial coordinate $x$ the deflected shape of the beam can be found analytically. Since the present case of deflection-independent loading is considered as a subsidiary problem, which is investigated in order to gain insight and establish a solution approach for the case of electrostatic loading, where a closed form solution is not available, we use the Galerkin method for the solution of Eq. (17) for the sake of consistency.

The reduced order model, Eq. (12), takes the form

$$(\mathbf{B} + \gamma\mathbf{M})(\mathbf{q} - \mathbf{q}_0) + \alpha(\mathbf{q}^{\mathbf{T}}\mathbf{S}\mathbf{q} - \mathbf{q}_0^{\mathbf{T}}\mathbf{S}\mathbf{q}_0)\mathbf{S}\mathbf{q} = -\beta^M\mathbf{p} \tag{19}$$

where the elements of the generalize force vector $\mathbf{p} = \{p_i\}$ and of the diagonal matrix $\mathbf{M} = [m_{ij}]$ are given by the expressions

$$p_i = \int_0^1 \varphi_i dx \quad m_{ij} = \delta_{ij}\int_0^1 \varphi_i\varphi_j dx \tag{20}$$

The analysis of the symmetric and the non-symmetric responses is carried out using the two degrees of freedom RO model described by the two coupled equations

$$(b_{11} + \gamma m_{11})(q_1 - h) + \alpha s_{11}^2\left(q_1^2 - h^2\right)q_1 + \alpha s_{11}s_{22}q_2^2 q_1 = -\beta^M p_1 \tag{21}$$

$$(b_{22} + \gamma m_{22})q_2 + \alpha s_{11}s_{22}\left(q_1^2 - h^2\right)q_2 + \alpha s_{22}^2 q_2^3 = 0 \tag{22}$$

where $m_{11} = 0.396,\ m_{22} = 0.439$ and $p_1 = 0.523$.

One of the advantages of the mechanically loaded beam model is that it can be treated analytically. The system (21) and (22) incorporates two cubic equations that, for a given $\beta^M$, may have one or three pairs of real solutions $(q_1, q_2)$, depending on $h$. One observes that Eq. (22) has an unconditional trivial solution $q_2 = 0$, which is associated with the symmetric deflection of the beam. The corresponding symmetric equilibrium curve $\beta^M = \beta^M(q_1)$ is obtained from Eq. (21) where $q_2 = 0$. The second group of solutions, corresponding to the non-symmetric buckling of the beam, is obtained by excluding the trivial equilibrium $q_2 = 0$ from Eqs. (22) and by solving the resulting quadratic equation in terms of $q_2$ to yield

$$q_2 = \pm\sqrt{-\frac{(\gamma m_{22} + b_{22})}{\alpha s_{22}^2} + \frac{s_{11}\left(h^2 - q_1^2\right)}{s_{22}}} \tag{23}$$

By substituting $q_2 = q_2(q_1)$ given by Eq. (23) into Eq. (21), we find $\beta^M = \beta^M(q_1)$ corresponding to the non-symmetric solutions. The procedure described above actually corresponds to a displacement control procedure of which both $q_2$ and $\beta^M$ are expressed in terms of the prescribed $q_1$. Note that the direct numerical solution of the system Eqs. (21) and (22) combined with the displacement control approach (prescribed $q_1$) was also implemented, mainly in order to lay grounds for the solution of the electromechanical problem, which cannot be solved analytically. The solver for nonlinear algebraic equations, which is a part of the Maple package was used. The results of the numerical and of analytical solutions were practically identical.

The results are presented in Fig. 2(a)–(d) where the bifurcation diagrams for different values of the initial elevation $h$ are shown. One observes that in the case of two DOF RO model, the equilibrium configurations can be presented by three-dimensional curves (bifurcation diagrams) in the space of $q_1, q_2, \beta^M$ (e.g., see Thompson and Hunt, 1973). The behavior of the beam is typical for curved arches (e.g., see Simitses and Hodges, 2006). Namely, for small $h$, the response is symmetric and without snap-through buckling, Fig. 2(a). For relatively small (but sufficient to have a snap-through) $h$, the response is symmetric and $q_2$ is zero, Fig. 2(b). However, the equilibrium curve corresponding to the symmetric response contains two limit points, $S$ and $R$, which are associated with the snap-through buckling and the release (snap-back), respectively. For larger initial elevations, two anti-symmetric responses with $q_2 \neq 0$ emerge from the bifurcation points $AS$ and $AR$, located on the unstable branch of the symmetric equilibrium curve, as can be seen in Fig. 2(c). Hereafter we refer to these points as the bifurcation or symmetry breaking points (the asymmetric snap-through point ($AS$) and the asymmetric release point ($AR$)). In this scenario, the stability of the beam is still defined by the limit point (symmetric snap-through and release) buckling as the bifurcation points are not reached under quasistatic loading. For even larger $h$, the bifurcation points are located on the stable branches of the symmetric equilibrium curve, Fig. 2(d). In this case, the stability of the beam is defined by the location of the bifurcation points since the non-symmetric snap-through and the non-symmetric release are reached before the limit point buckling and limit point release during the quasistatic loading and unloading, respectively.

One may conclude, that several buckling criteria can be established. The first one defines the minimal initial elevation necessary for the appearance of the limit points. The second is associated with the non-critical non-symmetric buckling emerging from the unstable symmetric branch of the equilibrium curve. Finally, the third one defines the threshold criterion sufficient for the appearance of the critical symmetry breaking, when the non-symmetric

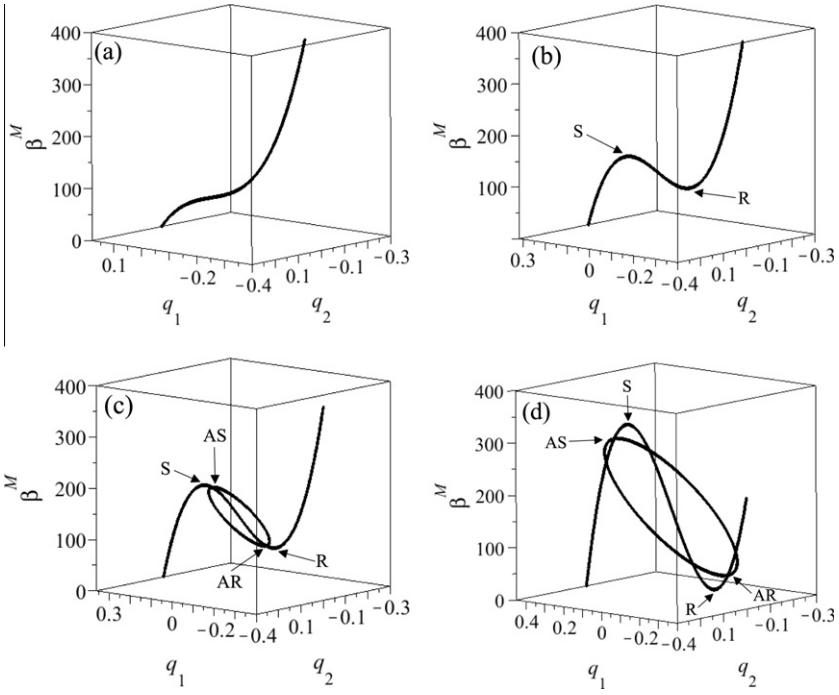


**Fig. 2.** Bifurcation diagram of the mechanically loaded beam on a linear elastic foundation (two DOF RO model, Eqs. (21) and (22)) for $d = 0.2$, $\gamma = 10$ and different initial elevations: (a) $h = 0.225$ (b) $h = 0.315$ (c) $h = 0.36$ (d) $h = 0.45$. Points *S* and *R* represent the symmetric snap-through and release limit points, respectively; points *AS* and *AR* represent the bifurcation points of the asymmetric snap-through and release, respectively.

snap-through takes place under a loading smaller than that corresponding to the limit-point value (e.g., see Simitses and Hodges, 2006 and Simitses, 1989).

### 4.2. Snap-through criteria

In the case of the mechanically loaded beam and linearly elastic foundation, the symmetry breaking criterion can be obtained directly from Eq. (23), by requiring that the expression under the square root is positive (i.e., that two real non-symmetric solutions of Eq. (22) exist). However, this approach is unapplicable in the case of the electrostatic loading when the generalized force appears in an integral form (see Eq. (13)). Since the bifurcation points are located on the equilibrium curve corresponding to the symmetric deflection (i.e, to $q_2 = 0$), we linearize Eqs. (21) and (22) around $q_2 = 0$ and obtain

$$(b_{11} + \gamma m_{11})(q_1 - h) + \alpha s_{11}^2\left(q_1^2 - h^2\right)q_1 = -\beta^M p_1 \tag{24}$$

$$\left(b_{22} + \gamma m_{22} + \alpha s_{11} s_{22}\left(q_1^2 - h^2\right)\right)q_2 = 0 \tag{25}$$

The first of Eq. (24), which is independent on $q_2$, describes the symmetric response of the beam, and is identical to a single degree of freedom model. The location of the limit points, which are the extremal points of the equilibrium curve $\beta^M = \beta^M(q_1)$ (see Eq. (24)), can be found from the condition $d\beta^M/dq_1 = 0$, which leads to the equation

$$3\alpha s_{11}^2 q_1^2 + b_{11} + \gamma m_{11} - \alpha s_{11}^2 h^2 = 0 \tag{26}$$

and corresponds to the appearance of an inflection point on the equilibrium curve. By solving Eq. (26) in terms of $q_1$, we obtain the values $q_S$ and $q_R$ corresponding to the limit point snap-through and release

$$q_S = \sqrt{\frac{h^2}{3} - \frac{b_{11} + \gamma m_{11}}{3\alpha s_{11}^2}} \quad q_R = -\sqrt{\frac{h^2}{3} - \frac{b_{11} + \gamma m_{11}}{3\alpha s_{11}^2}} \tag{27}$$

By requiring that both roots of Eq. (26) are real, i.e., that the expression under the square root in Eq. (27) is positive, we obtain the minimal value of the initial elevation, which is required for the appearance of the snap-through buckling

$$h \geqslant \frac{1}{s_{11}}\sqrt{\frac{b_{11} + \gamma m_{11}}{\alpha}} \tag{28}$$

Note that when $h$ has the critical value given by Eq. (28), we have $q_S = q_R = 0$ and the inflection point of the equilibrium curve corresponds to the straight configuration of the deformed beam. The dimensional counterpart of Eq. (28) for the case of a beam of rectangular cross-section, when $\alpha = 6/d^2$, is

$$\frac{\hat{h}}{\hat{d}} \geqslant \sqrt{\frac{b_{11}}{6s_{11}^2} + \frac{2m_{11}\hat{k}L^4}{s_{11}^2 \tilde{E}\hat{b}\hat{d}^3}} \tag{29}$$

One observes that the presence of a positive elastic foundation increases the value of $\hat{h}/\hat{d}$, which is required for bistability. Note also that in the absence of the elastic foundation, i.e., for $k = 0$, Eq. (29) yields $\hat{h}/\hat{d} \geqslant 1.179$ (see Krylov et al., 2008).

By requiring that Eq. (25) has a non-trivial solution $q_2 \neq 0$, namely that the expression in the parentheses is zero, we find the values of $q_1$ corresponding to the location of the bifurcation points on the symmetric equilibrium curve

$$q_{AS} = \sqrt{h^2 - \frac{b_{22} + \gamma m_{22}}{\alpha s_{11} s_{22}}} \quad q_{AR} = -\sqrt{h^2 - \frac{b_{22} + \gamma m_{22}}{\alpha s_{11} s_{22}}} \tag{30}$$

Then, by requiring that both $q_{AS}$ and $q_{AR}$ are real, i.e., Eq. (25) has two real roots in terms of $q_1$, we obtain the necessary condition for the appearance of the non-symmetric response

$$h \geqslant \sqrt{\frac{b_{22} + \gamma m_{22}}{\alpha s_{11} s_{22}}} \tag{31}$$

or, in the dimensional form (for beams of rectangular cross-section when $\alpha = 6/d^2$)

$$\frac{\hat{h}}{\hat{d}} \geqslant \sqrt{\frac{b_{22}}{6s_{11}s_{22}} + \frac{2m_{22}\hat{k}L^4}{s_{11}s_{22}\widetilde{E}\hat{b}\hat{d}^3}} \tag{32}$$

One observes that when $h$ reaches the limiting value given by Eq. (31), $q_{AS} = q_{AR} = 0$, such that the two coinciding bifurcation points correspond to the straight configuration of the deformed beam. In the absence of an elastic foundation we have $\hat{h}/\hat{d} \geqslant 1.680$. Similarly to the limit point snap-through criterion, Eq. (29), the presence of the elastic foundation increases the minimal value of $\hat{h}/\hat{d}$ required for the appearance of the non-symmetric buckling.

When the initial elevation of the beam exceeds the minimal value given by the criterion (32), the beam may manifest a non-symmetric buckling. However, the non-symmetric solutions emerge from the bifurcation points *AS* and *AR*, which are located on the unstable branches of the equilibrium curve and cannot be reached under the quasi static loading. The non-symmetric buckling becomes critical when the bifurcation occurs on the stable branch of the symmetric response curve given by Eq. (24). In order to define the sufficient condition for the critical (i.e., taking place under a loading smaller than that corresponding to the limit point) non-symmetric buckling, the relative position of the bifurcation points, *AS* and *AR*, with respect to the limit points, *S* and *R*, is examined.

Fig. 3 shows the values of $q_1$ corresponding to the limit points $q_S, q_R$, Eq. (27), and to the bifurcation points, $q_{AS}, q_{AR}$, Eq. (30), as a function of the initial elevation, for beams of rectangular cross-section with specific values of $d = 0.2$ and $\gamma = 10$. Since the non-symmetric buckling is critical when $q_{AS} \leqslant q_S$, the threshold criterion for the non-symmetric response is derived by requiring $q_S = q_{AS}$ (where $q_S$ and $q_{AS}$ are given by Eqs. (27) and (30), respectively). This results in the following sufficient condition for the critical non-symmetric bifurcation (note that since all the critical points are located symmetrically with respect to $q_1 = 0$, by requiring $q_{AR} = q_R$ the same criterion is obtained)

$$h \geqslant \sqrt{\frac{3(b_{22} + \gamma m_{22})}{2\alpha s_{11}s_{22}} - \frac{b_{11} + \gamma m_{11}}{2\alpha s_{11}^2}} \tag{33}$$

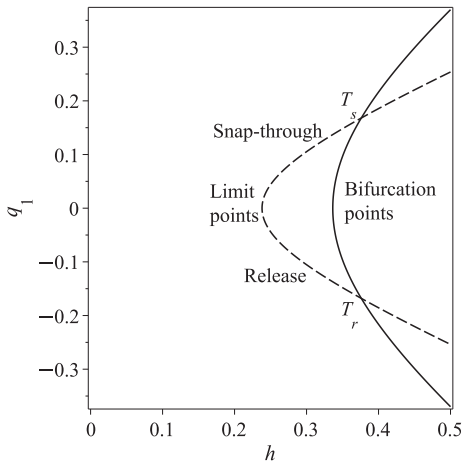


**Fig. 3.** Location of the critical points of the mechanically loaded beam with rectangular cross-section attached to an elastic foundation for $d = 0.2$, $\gamma = 10$ and varying $h$. The dashed line represents the limit points of the buckling diagram given by Eq. (27) and corresponding to the symmetric snap through (points *S*) and the symmetric release (points *R*). The solid line represents bifurcation points of the asymmetric snap-through (points *AS*) and asymmetric release (points *AR*) given by Eq. (30). Points $T_s$ and $T_r$ represent the threshold of the critical asymmetric snap-through and release points, respectively, where the bifurcation points coincide with the limit points.

The dimensional form of Eq. (33) is

$$\frac{\hat{h}}{\hat{d}} \geqslant \sqrt{\frac{b_{22}}{4s_{11}s_{22}} - \frac{b_{11}}{12s_{11}^2} + \frac{\hat{k}L^4}{\widehat{E}\hat{b}\hat{d}^3}\left(\frac{m_{11}}{s_{11}^2} + \frac{3m_{22}}{s_{11}s_{22}}\right)} \tag{34}$$

Note that in the absence of the elastic foundation, the non-symmetric bifurcation occurs when $\hat{h}/\hat{d} > 1.88$.

Fig. 3 suggests that it is not necessary to calculate the roots of Eq. (25) or its discriminant in a closed form in order to obtain the criterion (31). Namely, by calculating the derivative of Eq. (25) with respect to $q_1$ one finds that $dh/dq_1 = 0$ at $q_1 = 0$. Next, by expressing $h$ in terms of $q_1$ from Eq. (25) and then setting $q_1 = 0$ one obtains (31). This approach will be used for the analysis of the beam subject to the nonlinear electrostatic loading where closed form solutions of Eqs. (15) and (16) are not available. Similarly, by expressing $h^2$ in terms of $q_1$ from Eq. (26), equating it to $h^2$ from Eq. (25), and solving the resulting equation in terms of $q_1$ we obtain

$$q_1 = \pm\frac{1}{\sqrt{2\alpha}s_{11}}\sqrt{(b_{22} + \gamma m_{22})\frac{s_{11}}{s_{22}} - b_{11}} \tag{35}$$

which defines the location of the two critical bifurcation points (Fig. 3) in terms of $\gamma$ and $\alpha$. By substituting the expression for $q_1$ given by Eq. (35) back into Eq. (25), and solving it in terms of $h$, one obtains (33). In the case of a beam with a rectangular cross section we obtain

$$\frac{q_1}{d} = \pm\sqrt{\frac{b_{22} + \gamma m_{22}}{3s_{11}s_{22}} - \frac{b_{11}}{3s_{11}^2}} \tag{36}$$

This equation indicates that the bifurcation threshold points are located symmetrically with respect to $q_1 = 0$ and that their location depends linearly on $d$.

The graphical representations of all the three criteria – Eqs. (28), (31) and (33) are combined in Fig. 4. The curves separate the regions where the different buckling behavior-monotonous force–deflection characteristic, symmetric limit point buckling, noncritical and critical non-symmetric bifurcations-takes place. Analysis of the criteria Eqs. (28), (31), (33) and Fig. 4 shows, that the presence of the elastic foundation affects the buckling behavior and increases the value of the initial elevation required for the appearance of the corresponding buckling (see Simitses and Hodges, 2006). In the case of a negative foundation, the influence of which can be considered to be equivalent to that of the distributed electrostatic force (e.g. see Elata and Abu-Salih, 2006; Krylov, 2008) the critical values of $h$ decrease and the structure is more prone to the limit point and non-symmetric buckling. The criteria for the case of a negative foundation can be obtained directly from Eqs. (28), (31) and (33) by changing the sign of the elastic foundation parameter $\gamma$.

By considering the snap-through criteria, Eqs. (28), (31) and (33) and Fig. 4 one observes that in the case of a negative elastic foundation the limit point and non-symmetric buckling are possible even in the case of an initially straight beam. The physical meaning of these instabilities is related to the fact that the presence of a negative elastic foundation, which can be viewed as an actuator, introduces an additional instability mechanism. For example, in the case of a straight beam, the critical value $\gamma = -b_{11}/m_{11}$ of the elastic foundation parameter (such that the expression under the square root in Eq. (28) becomes negative and the solid line in Fig. 4 crosses the axis $h/d = 0$) corresponds to the symmetric, fundamental mode, limit point buckling of the beam. The value $\gamma = -b_{22}/m_{22}$ (see Eq. (31) and the dotted line in Fig. 4) is associated with the second, non-symmetric bifurcation mode of an initially straight beam on a negative elastic foundation. Note that this scenario can be realized by actuating the straight beam by two electrodes symmetrically located at two sides of it

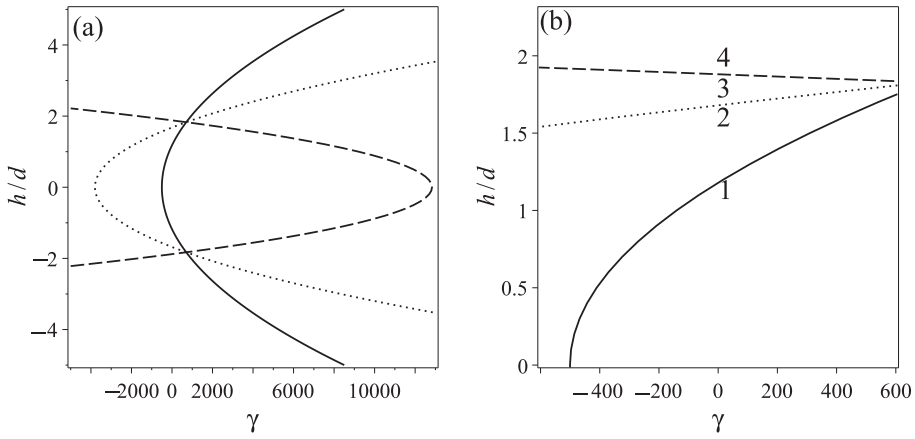


**Fig. 4.** The dependence of the relative critical initial elevations on the elastic foundation parameter as given by the three criteria in Eqs. (28) (solid line), (31) (doted line) and (33) (dashed line) (for a square crosssection). (b) A focus on the region of moderate foundation's stiffness given in (a). Typical responses in regions 1, 2, 3 and 4 are shown by Fig. 2(a), (b), (c) and (d), respectively.

(e.g. see Elata and Abu-Salih, 2006; Krylov, 2007; Krylov, 2008). In the case of a positive foundation, the non-symmetric buckling is possible if the stiffness of the foundation is high with respect to the bending stiffness of the beam. It follows from considering of Eqs. (28), (31) and (33) that all three curves cross at the same point at $\gamma = (m_{11}s_{22} - m_{22}s_{11})/(b_{22}s_{11} - b_{11}s_{22})$. Note that in the case of the elastic foundation with high positive stiffness the contribution of the high-symmetric and non-symmetric-buckling modes should be taken into consideration and the two DOF model could be inadequate. Since we are interested in the analysis of electrostatically actuated beams where the influence of the initial curvature is dominant and the elastic foundation is actually negative, the analysis of the case of the elastic foundation with high stiffness is out of the scope of this work. A focus on the region corresponding to the moderate positive and negative $\gamma$ is shown in Fig. 4(b).

To summarize this section, one may conclude that the presence of a linear elastic foundation affects the buckling behavior of the beam as reflected in both the limit point snap-through and the symmetry breaking criteria. Based on these results, one may expect that the distributed nonlinear displacement-dependent force may have a similar influence on the symmetry breaking of the beam as will be demonstrated in the next section.

## 5. Electrostatic loading

In the case of the electrostatic loading, Eqs. (15) and (16) corresponding to the two DOF model, cannot be solved in a closed form due to the presence of the integral terms, which are associated with the electrostatic force. For this reason, three-dimensional bifurcation diagrams, mapping all the stable and unstable equilibrium configurations in the $q_1, q_2, \beta$ space are built numerically. First, the voltage parameter $\beta$ is expressed in terms of $q_1, q_2$ using each of Eqs. (15) and (16). Equilibrating these expressions, we obtain a nonlinear algebraic equation $\mathcal{F}(q_1, q_2) = 0$, which implicitly relates $q_1$ and $q_2$. By prescribing the values of $q_1$ (displacement control), we solve the equation $\mathcal{F}(q_1, q_2) = 0$ numerically, using the solver for nonlinear algebraic equations incorporated into the Maple package, and obtain $q_2 = q_2(q_1)$. The integrals are evaluated numerically. Finally, the values of the voltage parameter $\beta$, corresponding to the symmetric and non-symmetric branches of the bifurcation diagram are obtained by substituting the values of $q_1$ and $q_2(q_1)$ back into Eq. (15).

The result is presented in Fig. 5, which is the counterpart of Fig. 2, illustrating the response of a mechanically loaded beam on a linearly elastic foundation. The expected similarity between the figures implies that the criteria for the symmetric snap-through and both non-critical (necessary condition) and critical (sufficient condition) bifurcations should be defined also in the case of the electrostatic loading. However, in contrast to the case of the mechanical, deflection-independent loading, the presence of the nonlinear electrostatic force results in the appearance of an additional limit point on the bifurcation diagram (point *PI*), so-called pull-in instability (see Das and Batra, 2009a; Krylov et al., 2008; Zhang et al., 2007).

### 5.1. Snap-through criteria

In accordance with Fig. 5 and similarly to the case of the mechanically loaded beam, the branches of the bifurcation diagram corresponding to the non-symmetric configurations of the electrostatically loaded beam emerge from the equilibrium path representing the symmetric response. Hence, in order to find the position of the bifurcation points on the symmetric branch we first linearize Eqs. (15) and (16) around the path $q_2 = 0$. Taking into account that the following integrals vanish

$$\int_0^1 \frac{\varphi_1\varphi_2}{(1+q_1\varphi_1)^3}dx = 0 \quad \int_0^1 \frac{\varphi_2}{(1+q_1\varphi_1)^2}dx = 0 \tag{37}$$

we obtain

$$b_{11}(q_1 - h) + \alpha s_{11}^2\left(q_1^2 - h^2\right)q_1 + \beta I_1(q_1) = 0 \tag{38}$$

$$\left(b_{22} + \alpha s_{11}s_{22}\left(q_1^2 - h^2\right) - 2\beta I_2(q_1)\right)q_2 = 0 \tag{39}$$

where

$$I_1(q_1) = \int_0^1 \frac{\varphi_1}{(1+q_1\varphi_1)^2}dx \quad I_2(q_1) = \int_0^1 \frac{\varphi_2^2}{(1+q_1\varphi_1)^3}dx \tag{40}$$

Eq. (38) is independent on $q_2$ and is identical to Eq. (19) with $n = 1$, it is to say, it corresponds to the single DOF model and describes the symmetric response of the beam. By expressing $\beta$ in terms of $q_1$ using Eq. (38), differentiating it with respect to $q_1$ and taking into account that $I_1 > 0$ for $q_1 > -1$, we obtain the equation

$$\alpha s_{11}^2 q_1^2(I_3q_1 - 3I_1) + (I_3q_1 - I_1)(b_{11} - \alpha s_{11}^2 h^2) - b_{11}I_3h = 0 \tag{41}$$

whose roots $q_S, q_R, q_{PI}$ correspond to the symmetric snap-through, symmetric release and pull-in points of the bifurcation diagram, respectively. Here $I_3 = dI_1/dq_1$. The dependence between the location of the roots $q_S, q_R, q_{PI}$ of Eq. (41) and the initial elevation of

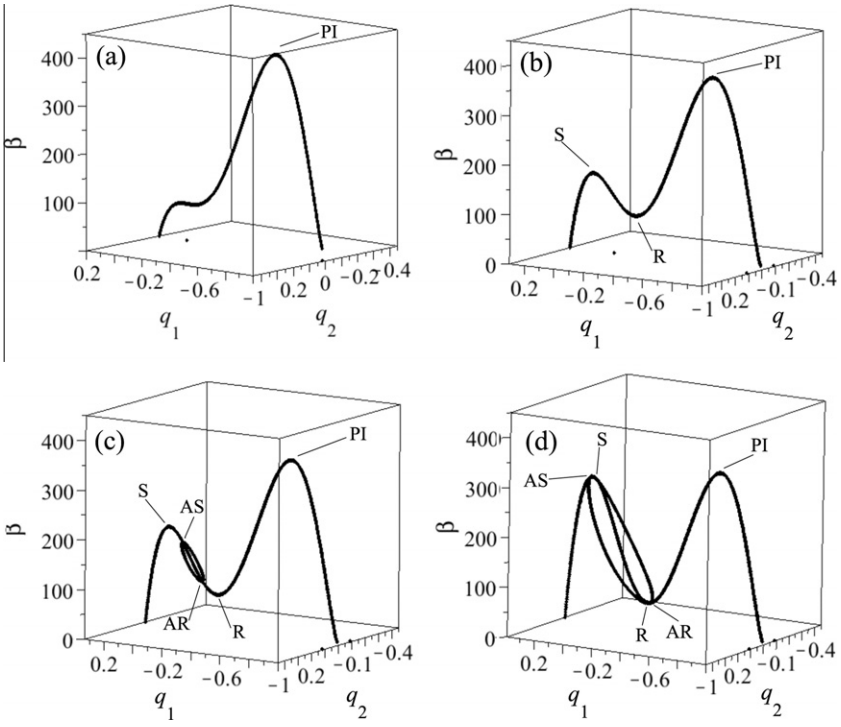


**Fig. 5.** Bifurcation diagram of the electrostatically loaded beam (two DOF RO model, Eqs. (15) and (16)) for $d = 0.2$ and different initial elevations elevations: (a) $h = 1$, (b) $h = 0.3$, (c) $h = 0.332$, (d) $h = 0.386$. Point *S* and *R* are the snap-through and release limit points; points *AS* and *AR* are the bifurcation points of the snap-through and release and point *PI* is the pull-in point.

the beam, $h$, (for a prescribed value of $\alpha$) is shown in Fig. 6(a) and (b) for two values of $d$. The corresponding critical values of the voltage parameter are shown in Fig. 6(c) and (d).

In order to obtain the symmetric snap-through criterion, we note that Eq. (41) is quadratic in $h$ and can be solved to obtain $h(q_1)$. The minimum of $h(q_1)$ is found (for a given $\alpha$ which is considered as a parameter) by solving numerically $dh(q_1)/dq_1 = 0$. This yields the value of $q_1$ (which depends solely on $\alpha$) corresponding to the minimum of the curve $h = h(q_1)$ on Fig. 6. The snap-through criterion, namely, the minimal value of $h$ required to have the snap-through, can be obtained by substituting this value of $q_1$ back into the solution $h(q_1)$ of Eq. (41). The dependence of the ratio $h/d$ on the relative thickness $d = \dot{a}/g_0$ of a beam of a rectangular cross section (when $\alpha = 6/d^2$) is shown by solid line No. 1 in Fig. 7.

Fig. 6 indicates that the minimum of the curve $h = h(q_1)$ defining the necessary condition of the symmetric snap-through is located at small (but not zero, in contrast to the case of a mechanical force, Eqs. (27) and (28)) $q_1$. This suggests that an approximation for the snap-through criterion can be obtained by replacing the curve $h = h(q_1)$ in the vicinity of $q_1 = 0$ by a simple polynomial (quadratic) expression and consequently, the derivative $dh/dq_1$ by a linear function. Hence, we linearize the derivative $dh/dq_1$, solve it in terms of $q_1$, substitute the result back into the dependence $h = h(q_1)$ (obtained from Eq. (41)) and then expand it into Taylor series up to quadratic order. As a result, we obtain the simple approximation for the symmetric snap-through criterion

$$\frac{h}{d} > \sqrt{\frac{b_{11}}{6s_{11}^2}}\left(1 - \frac{m_{11}}{p_1}\sqrt{\frac{b_{11}}{6s_{11}^2}}d\right) \tag{42}$$

Note that Eq. (42) is in excellent agreement with the approximate symmetric snap-through criterion first obtained in Krylov et al. (2008) using a different approach. Note also that the value $\sqrt{b_{11}/6s_{11}^2}$ is the value corresponding to the case of a curved beam under uniform deflection-independent loading. For the base functions adopted in this work, we obtain

$$\frac{h}{d} > 1.179 - 1.054d \tag{43}$$

Consider now the criteria for the non-symmetric snap-through. By expressing $\beta$ in terms of $q_1$ using Eq. (38) and by substituting this expression into Eq. (39), we obtain that the eigenvalue problem (39) has a non-trivial solution when the following equation is satisfied

$$2I_2(q_1 - h)(b_{11} + \alpha s_{11}^2 q_1(q_1 + h)) + I_1\left(b_{22} - \alpha s_{11}s_{22}(q_1^2 - h^2)\right) = 0 \tag{44}$$

The roots of Eq. (44) define the location of the bifurcation points along the equilibrium path corresponding to the symmetric response. The location of these points depends on two geometric parameters of the beam, namely $\alpha$ (and therefore $d$) and $h$ and is shown by the solid lines in Fig. 6. One observes that two non symmetric bifurcation criteria can be formulated. The first defines the condition required for the appearance of the bifurcation (the necessary condition) whereas the second defines the geometrical requirements for the appearance of bifurcation point on the stable branch of the symmetric response (the sufficient condition). Recall that in the last case the bifurcation is critical in the sense that the non-symmetric buckling takes place at values of the loading that are smaller than those corresponding to the symmetric limit point snap-through buckling. Note also that in contrast to the snap-through and bifurcation points, which appear only when the initial elevation is higher than certain value, the presence of the electrostatic pull-in instability is unconditional.

The necessary condition is obtained using Eq. (44), which corresponds to the bifurcation points, shown by the dashed lines in Fig. 6. Note that due to the presence of the integrals $I_1$ and $I_2$, Eq. (44) is not polynomial as in the case of the linearly elastic

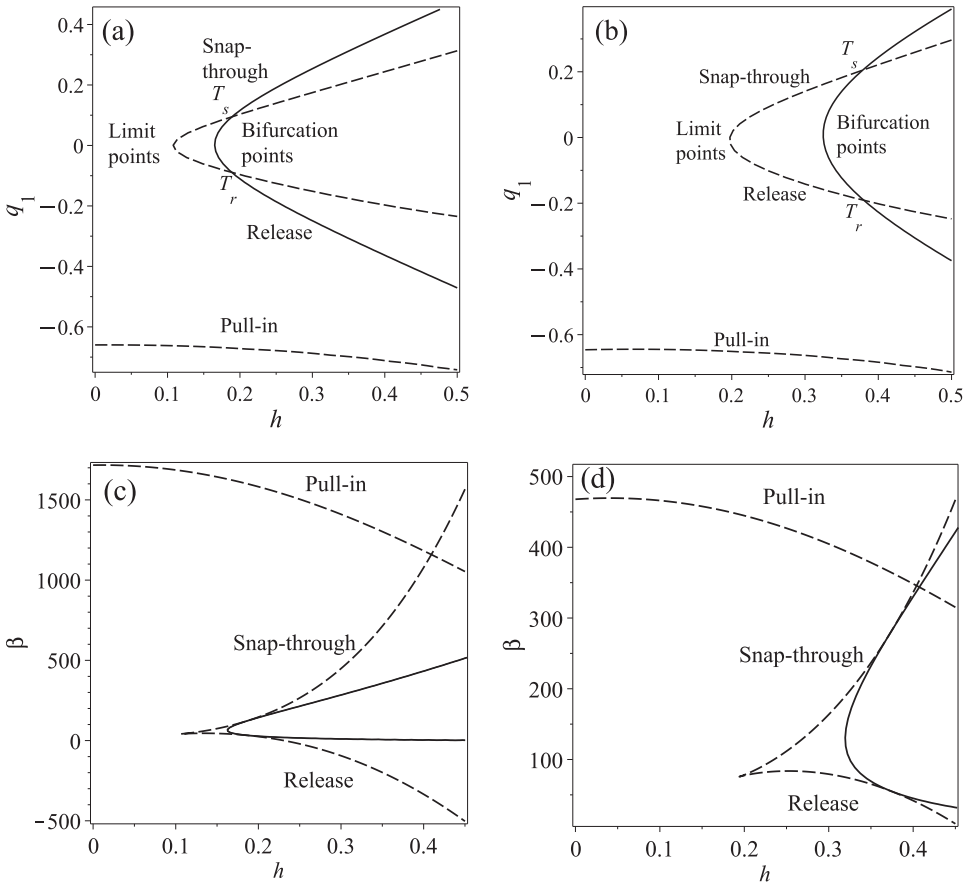


**Fig. 6.** (a), (b) Location of the critical points of the electrostatically loaded beam with rectangular cross-section and (c), (d) corresponding critical values of the voltage parameter for: (a) (c) $d = 0.1$ and (b) (d) $d = 0.2$ and varying $h$. The dashed lines represent the limit points of the buckling diagram given by Eq. (41) and corresponding to the symmetric snap through (point *S*), the symmetric release (point *R*) and the pull-in (point *PI*). The solid lines represent bifurcation points of the asymmetric snap-through (point *AS*) and asymmetric release (point *AR*) given by Eq. (44). Points $T_s$ and $T_r$ represent the threshold of the critical asymmetric snap-through and release points, respectively, where the bifurcation points coincide with the limit points.

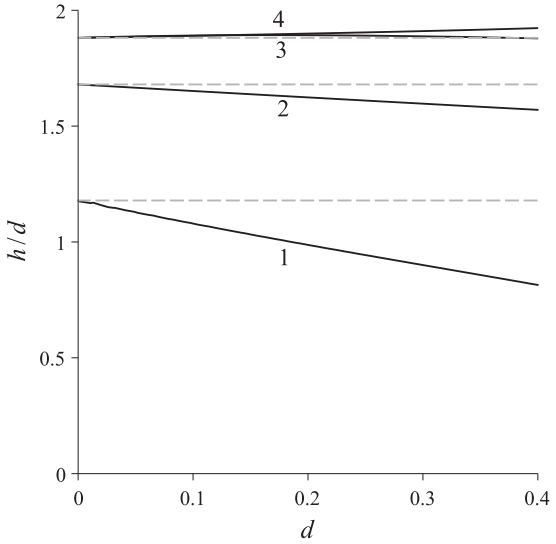


**Fig. 7.** Phase diagram of the symmetrical and non-symmetrical snap-through criteria. The black solid lines represent the criteria for the electrostatically loaded beam, and the dashed gray lines represent the criteria for a mechanically loaded beam. Solid line No. 1 is the necessary criterion given by Eq. (43); line 2 represents the necessary condition for the appearance of an asymmetrical snap-through given by Eq. (45); lines 3 and 4 corresponds to the sufficient conditions for the snap-through and release bifurcation points respectively given by Eqs. (47) & (48), respectively.

foundation (see Eq. (26)), and cannot be solved in a closed form. However, this equation is quadratic in $h$. Hence, the non-critical bifurcation criteria is obtained by finding the minimum of the curve $h = h(q_1)$ extracted from Eq. (44) (with $\alpha$ considered to be a parameter), following the approach used for the derivation of the symmetric snap-through criterion from Eq. (39). As a result we obtain, for a given $\alpha$ and therefore for a given relative thickness of the beam $d = \hat{d}/g_0$, the value of the initial elevation $h = \hat{h}/g_0$ required for the appearance of the non-symmetric bifurcation. We emphasize that, similarly to the symmetric buckling, the influence of the nonlinear electrostatic force on the symmetry breaking criterion manifests itself through the dependence of the result on the electrostatic gap $g_0$. The curve $h/d$ as a function of $d$ is shown by solid line No. 2 in Fig. 7.

Similarly to the approach used for the approximation of the symmetric snap-through criterion, we linearize the equation $dh/dq_1 = 0$ for small $q_1$ (see Fig. 6), solve it in terms of $q_1$ and obtain the approximation for the necessary criterion of the non-symmetric snap-through

$$\frac{h}{d} > \sqrt{\frac{b_{22}}{6s_{11}s_{22}}}\left(1 - \frac{b_{11}m_{22}}{p_1}\sqrt{\frac{1}{6s_{11}s_{22}b_{22}}}d\right) \tag{45}$$

or, for the adopted base functions,

$$\frac{h}{d} > 1.680 - 0.312d \tag{46}$$

In order to formulate the sufficient conditions for the non-symmetric snap-through and non-symmetric release, the points of intersection between the curve corresponding to the limit points and the curve associated with the points of bifurcation (threshold points $T_s$ and $T_r$ on Fig. 6) have to be found. This is achieved by extracting from both Eqs. (44) and (41) an expression for $h(q_1,\alpha)$. Equalization of these two expressions results in an implicit relation between $\alpha$ and the beam's midpoint elevations $q_1$ corresponding to the threshold points. For a given $\alpha$, the numerical solution of this equation provides two values of $q_1$, which, when substituted back into the solution $h(q_1,\alpha)$ of Eq. (44) or (41) yield the threshold values of $h$ which are sufficient for the appearance of the critical non-symmetric snap-through and non-symmetric release. The dependence between these values of $h$ and the thickness of the beam $d$ is shown by lines 3, 4 in Fig. 7.

It is worth noting, that in contrast to the case of the mechanical deflection-independent loading, in the case of the electrostatic force, the location $q_1(d)$ of the points corresponding to the critical non-symmetric snap-through and non-symmetric release is not symmetric with respect to $q_1 = 0$. Consequently, two different sufficient criteria should be formulated: one for the critical non-symmetric snap-through and another for the critical non-symmetric release. The validity of the present analysis for high values of $d$ and $h$, namely for setups in which the electrode is placed closer to the beam, is in question. This is due to the possible presence of higher modes of buckling, which become emanate when the distance between the electrode and the beam's edges is very small in relation to the distance between the electrode and the beam's center. This phenomenon was observed in Krylov and Seretensky (2006) for a membrane, which can be considered a special reduction of the present problem. Looping behavior of the electrostatically loaded curved beam of relatively high initial elevations was illustrated numerically in Das and Batra (2009b).

Since the sufficient criterion for the symmetry breaking cannot be obtained in a closed form, simple approximate expression describing the dependence between the $h/d$ ratio and $d$ were obtained by fitting the numerically obtained values using polynomial fits

$$\frac{h}{d} > 1.881 + 0.154d - 0.585d^2 + 0.539d^3 - 0.189d^4 \quad \text{(sufficient snap} - \text{through)} \tag{47}$$

$$\frac{h}{d} > 1.881 + 0.089d + 0.746d^4 - 2.065d^5 + 2.117d^6 \quad \text{(sufficient release)} \tag{48}$$

Fig. 7 reveals that the necessary condition, which is above the symmetric snap-through condition, is a lower-bound criterion for bifurcation. As for a certain range of $d$, the sufficient snap-through condition is below the sufficient release condition, suggesting that an asymmetric snap-through followed by a symmetric release can occur. The dependency of the criteria on $d$, namely on the stiffness of the system as defined by both the thickness of the beam and the gap, is qualitatively similar to the behavior of a curved beam on an elastic substrate subjected to mechanical load, which was analytically investigated in the previous section.

### 5.2. Numerical validation

The limit point snap-through and symmetry breaking criteria obtained in the previous section were developed using an approximate two degrees of freedom RO model. In order to validate the applicability of these criteria and estimate their accuracy, Eqs. (6) and (7) governing the behavior of the beam were solved numerically. Two different tools were used for this purpose: the boundary value problem solver, which is a part of the MAPLE package Maplesoft (2011) and a collocation-based boundary value problem solver bvp4c implemented in MATLAB (see Shampine et al., 2011). Note that it was chosen to solve the system of Eqs. (6) and (7) instead of the single integro-differential Eq. (8), which is less convenient for the direct numerical solution (numerical solutions of Eqs. (6) and (8) is discussed in more details in Krylov et al. (2008) and Krylov et al. (2011)).

Since we are interested in the analysis of the symmetry breaking in the structures under investigation, the initial configuration of the beams was taken to incorporate a small initial imperfection. The initial shape of the beams was taken to be a combination of the first, symmetric, and the second, anti-symmetric, vibrational modes of a straight beam

$$w_0(x) = h\varphi_1(x) + \delta\varphi_2(x) \tag{49}$$

with $\delta$ being the amplitude of the imperfection. A value of $\delta = \hat{\delta}/g_0 = 0.001$ was used in all the calculations.

First, the accuracy of the two DOF RO model was estimated. The comparison between the RO model and the numerical solution is illustrated in Fig. 8 where the dependence between the midpoint deflection of the beam and the applied voltage is shown. In the framework of the force control approach, which reflects an actual typical physical experiment (Krylov et al., 2011; Zhang et al., 2007), the voltage applied to the electrode was prescribed and was increased incrementally and the deflected shape of the beam was found at each increment. Note that only stable branches of the response curve can be tracked by this approach. In order to get as close as possible to the limit or bifurcation points characterized by the decreasing slope of the response curve, smaller load increments were used in the vicinity of the critical points.

Fig. 8 shows that for the adopted parameters of the beam (which are consistent with the realistic values used in the experiments of Krylov et al. (2008)), the two DOF RO model provides a reasonable accuracy. The RO model accuracy slightly decreases with the increasing voltage parameter. Specifically, a relative error of 0.01% in the critical voltage was observed at the snap-through point of the beam with $d = 0.2$ and $h = 0.332$, Fig. 8(a); errors of 4.1% and 8.1% in the critical voltages were obtained at the bifurcation and the pull-in points, respectively, of the beam with $d = 0.2$ and $h = 0.386$, Fig. 8(b). Note that errors of the same magnitude were reported in Krylov et al. (2008).

In order to quantify the level of the asymmetry of the deformed shape of the beam, we introduce an asymmetry measure based on the internal product between the deformed configuration of the beam and the second (anti-symmetric) base function $\varphi_2$

$$I = \int_0^1 (w - w_0)\varphi_2 dx \tag{50}$$

which increases as the asymmetry increases. A comparison between the orthogonality at the point suspected to be a limit snap-through of beam (a), $I^{(S)}$, and the orthogonality at the point suspected to be a bifurcation snap-through of beam (b), $I^{(\hat{A}S)}$, reveals that the latter is 3.8 times larger than the first. Similarly, $I^{(AR)}$ at the bifurcation release point of beam (b) is 3 times larger than $I^{(R)}$ at the limit release point of beam (a). This assists the above identification of the various critical points.

In addition, a displacement control procedure was used to track both stable and unstable responses together with the corresponding shapes of the deformed beam. In the framework of this approach, the problem was considered as a multipoint boundary value problem (Shampine et al., 2011). The deflection of the midpoint of the beam was prescribed along with the continuity conditions at this point (and without enforcing the symmetry at the midpoint). The voltage parameter and the deformed shape of the

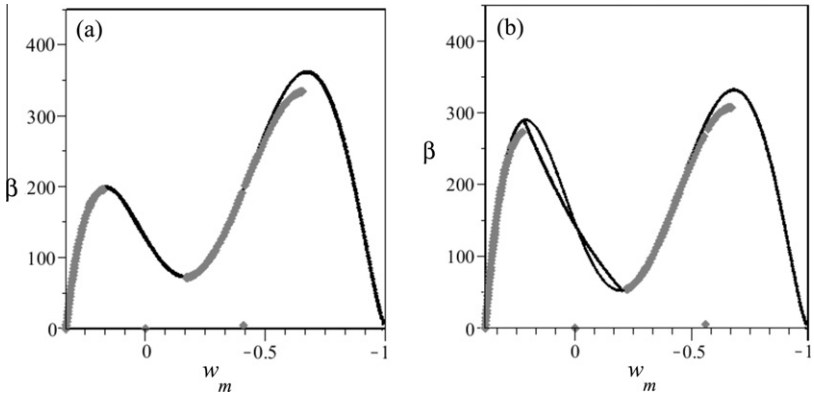


**Fig. 8.** Buckling diagram ($w_M$-midpoint elevation) for beams with $d = 0.2$ and (a) $h = 0.332$ (b) $h = 0.386$. Results of the RO model (black lines) and the force control numerical analysis (gray lines) are shown.

beam were found by means of a relaxation procedure using the solver bvp4c implemented in MATLAB used by Krylov et al. (2011) (see Bochobza-Degani et al., 2002 for the case of initially straight beam and the symmetric response). Note that while the displacement control approach adopted in this work may have a limited applicability for the analysis of the beams with higher initial elevations or larger relative thickness $\hat{d}/g_0$ where the contribution of higher symmetric modes may lead to looping behavior (Das and Batra, 2009b, see also Krylov and Seretensky, 2006 for the case of an elastic string), it is suitable for the analysis of beams of relatively small initial elevations. To ensure that the contribution of the higher modes is not pronounced for the considered configurations of the beam, the results obtained by the displacement control were compared with the results of the force control analysis, which describes the actual behavior of the beam up to the first instability point. An excellent agreement between the two approaches was observed.

The results for beams of three different initial elevations are shown in Fig. 9. Note that in order to highlight the correspondence between the points on the equilibrium curve of the beam and its deformed configurations, rotated plots of the voltage-deflection dependence are shown. The initial elevations of the beams were chosen in such a way that they fall within three different regions of the phase diagram (the initial elevation $h$ vs. the beam's thickness $d$, Fig. 7) defining the buckling behavior. The initial shape of the beam included a small imperfection such that it is given by two terms of Eq. (11) with $q_{02} = 0.001h$. As the point defining the geometric properties of the beam is placed above the snap-through criterion and below the necessary condition for bifurcation, region 2 in Fig. 7, the beam manifests the symmetric limit point snap-through buckling, Fig. 9(a). The beam with parameters corresponding to region 3 on Fig. 7, placed above the necessary and bellow the sufficient conditions of the symmetry breaking, exhibits a non-symmetric buckling with bifurcation points that are located on the unstable branch of the symmetric curve, Fig. 9(b). Fig. 9(c) illustrates the response of the beam with an initial elevation which is above the sufficient condition of the symmetry breaking, region 4 in Fig. 7. A non-symmetric response is clearly observed in this case.

Finally, we compare the location of the snap-through, release and pull-in points extracted from the direct numerical analysis (combined with the force control approach) with the values provided by the two DOF RO model, Fig. 6. The result of this comparison, performed for beams of different initial elevations, is shown in Fig. 10. Note that starting from a certain elevation $h$ the (symmetric and non-symmetric) snap-through voltage becomes higher than the pull-in value (Krylov et al., 2008). In this case the pull-in

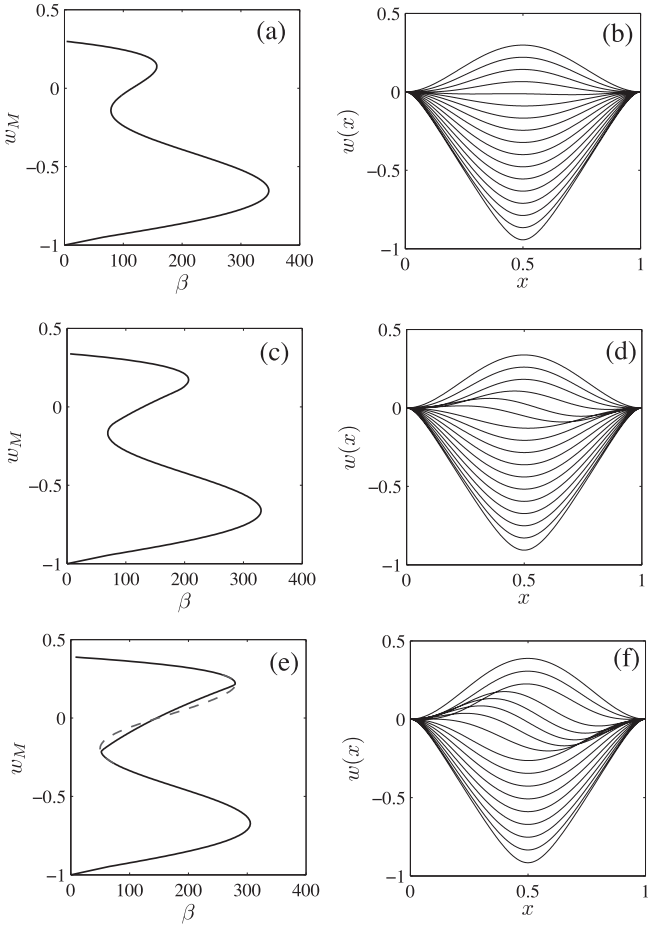


**Fig. 9.** (a), (c), (e) Bifurcation diagrams ($w_M$-midpoint elevation) and (b), (d), (f) the corresponding snapshots of the deformed shape of the beam during the loading for $d = 0.2$ and different initial elevations of the beam: (a), (b) $h = 0.3$ (region 2 in Fig. 7); (c), (d) $h = 0.34$ (region 3 in Fig. 7); (e), (f) $h = 0.39$ (region 4 in Fig. 7). Dashed line corresponds to the solution obtained under the symmetry conditions enforced at the midpoint.

and release configurations cannot be described using the force control algorithm and only the configurations corresponding to the snap-through points can be obtained. Fig. 10 indicates that the approximate and numerical values are in a good agreement. The deviation of the snap-through points from the curve corresponding to the symmetric response is clearly observed. One may conclude therefore that the approximate criteria obtained in this work can

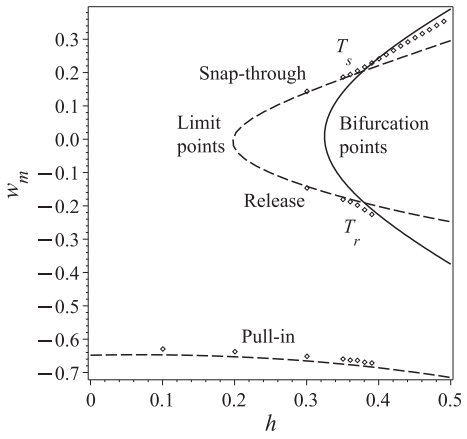


**Fig. 10.** Location of the midpoint of the beam corresponding to the snap-through, release and pull-in points and extracted via the numerical force control analysis (circles) for a beam of $d = 0.2$. Dashed line depicts the limit-points and the solid line depicts the bifurcation points resulting from the ROM Eqs. (41) and (44), respectively.

be used for the prediction of the symmetry breaking in electrostatically actuated curved micro beams.

## 6. Conclusions

In this work, the non-symmetric buckling of an initially curved beam loaded by a nonlinear, configuration dependent, electrostatic force was analyzed. The initial curved shape of the beam is provided by fabrication rather than by a pre-buckling and the beam is initially stress-free. The approximate reduced order model of the beam was built by means of Galerkin decomposition with linear undamped eigenmodes of an associated straight beam as base functions. Then, the criterion of a symmetric limit point snap-through buckling along with the criteria for a non-symmetric buckling were developed using the RO model limited to two-one symmetric and one skew-symmetric – DOF. The verification of the obtained results, using direct numerical solutions of the differential equations governing the beam's behavior, indicates that the established criteria can be used for the prediction of the symmetry breaking in electrostatically actuated curved micro beams with satisfactory accuracy.

Since the bifurcation points associated with the non-symmetric buckling may be located on stable or unstable branches of the symmetric equilibrium curve, depending on the beam's geometry parameters, two symmetry breaking criteria were established. The necessary non-symmetric buckling criterion provides the conditions required for the appearance of non-symmetric solutions which may emerge from points located on an unstable branch of the symmetric buckling path. In such a case, these non-symmetric configurations are not realized under quasi static force control loading, as in actual physical experiment, and the bifurcation conditions are not critical in a sense that the instability collapse takes place through the limit-point snap-through mechanism. In contrast, the sufficient symmetry breaking criterion establishes the condition for the critical non-symmetric buckling, when the bifurcation takes place at loading and deflection smaller than the limit-point snap-through buckling values.

In contrast to the case of mechanical, deflection independent loading, the nonlinearity of the electrostatic force, parameterized by the relative distance between the beam and the electrode, has a significant influence on both the symmetric and the non-symmetric buckling criteria. Specifically, the minimal values of the initial curvature/initial midpoint elevation of the beam required for the appearance of the instabilities are lower than in the mechanical case and the electrostatically loaded beams are more prone to the limit point and non-symmetric buckling. Note that each one of the criteria coincides with its mechanical counterpart when the distance between the beam and the electrode is large enough (compared to the beam's height and the critical values of the displacements) and when the nonlinearity of the electrostatic force is not pronounced. However, it was found that the symmetry breaking criteria are less affected by the electrostatic force when compared to the limit-point snap-through conditions. Consequently, for practical purposes, the common mechanical criterion can be used for the prediction of the critical non-symmetric buckling of electrostatically actuated shallow micro beams.

It is worth noting, that the results presented in this work are obtained for shallow beams with moderate initial elevations for which the distance between the beam and the electrode is not too small. When the distance between the beam and the electrode is comparable or smaller than the initial elevation of the beam (and therefore the critical snap-through and bifurcation values of the displacements), the contribution of the terms of the RO model associated with higher symmetric and non-symmetric base functions could be significant and the results obtained using the two DOF model could be inaccurate. The analysis of the behavior of deep beams is planned as a part of our future research.

## Acknowledgments

The authors thank Prof. J. Aboudi for fruitful discussions. The research is supported by The Israel Science Foundation (ISF, Grant No. 1426/08).

## References

Batra, R.C., Porfiri, M., Spinello, D., 2006. Analysis of electrostatic MEMS using meshless local Petrov–Galerkin (MLPG) method. Engineering Analysis with Boundary Elements 30, 949–962.

Batra, R.C., Porfiri, M., Spinello, D., 2007a. Effects of Casimir force on pull-in instability in micromembranes. Europhysics Letters 77, 20010.

Batra, R.C., Porfiri, M., Spinello, D., 2007b. Review of modeling electrostatically actuated microelectromechanical systems. Smart Materials and Structures 16, R23–R31.

Bažant, Z.P., Cedolin, L., 1991. Stability of Structures. Elastic, Inelastic, Fracture and Damage Theories. Dover Publications Inc., Mineola, New-York.

Bochobza-Degani, O., Elata, D., Nemirovsky, Y., 2002. An efficient DIPIE algorithm for CAD of electrostatically actuated MEMS devices. Journal of Microelectromechanical Systems 11, 612–620.

Charlot, B., Sun, W., Yamashita, K., Fujita, H., Toshiyoshi, H., 2008. Bistable nanowire for micromechanical memory. Journal of Micromechanics and Microengineering 18 (article number 045005).

Chen, J.S., Chang, D.W., 2007. Snapping of a shallow arch with harmonic excitation at one end. Journal of Applied Mechanics 129, 514–519.

Das, K., Batra, R.C., 2009a. Pull-in and snap-through instabilities in transient deformations of microelectromechanical systems. Journal of Micromechanics and Microengineering 19, article number 035008.

Das, K., Batra, R.C., 2009b. Symmetry breaking, snap-through and pull-in instabilities under dynamic loading of microelectromechanical shallow arches. Smart Materials and Structures 18, article number 115008.

Dym, C.L., 1974. Stability Theory and Its Applications to Structural Mechanics. Noordhoff Pub, Groningen.

Elata, D., Abu-Salih, S., 2006. Analysis of electromechanical buckling of a prestressed microbeam that is bonded to an elastic foundation. Journal of Mechanics Of Materials And Structures 1, 911–923.

Intaraprasonk, V., Fan, S., 2011. Nonvolatile bistable all-optical switch from mechanical buckling. Applied Physics Letters 98, article number 241104.

Krylov, S., 2007. Lyapunov exponents as a criterion for the dynamic pull-in instability of electrostatically actuated microstructures. International Journal of Non-Linear Mechanics 42, 626–642.

Krylov, S., 2008. Parametric excitation and stabilization of electrostatically actuated microstructures. International Journal for Multiscale Computational Engineering 6, 563–584.

Krylov, S., Seretensky, S., 2006. Higher order correction of electrostatic pressure and it's influence on the pull-in behavior of microstructures. Journal of Micromechanics and Microengineering 16, 1382–1396.

Krylov, S., Ilic, B., Schreiber, D., Seretensky, S., Craighead, H., 2008. The pull-in behavior of electrostatically actuated bistable microstructures. Journal of Micromechanics and Microengineering 18, 055026.

Krylov, S., Ilic, B.R., Lulinsky, S., 2011. Bistability of curved micro beams actuated by fringing electrostatic fields. Nonlinear Dynamics 66, 403–426.
Mallon, N., Fey, R., Nijmeijer, H., Zhang, G., 2006. Dynamic buckling of a shallow arch under shock loading considering the effects of the arch shape. International Journal of Non-Linear Mechanics 41, 1057–1067.
Maplesoft, A division of Waterloo Maple Inc., 2011. dsolve/numeric/BVP-find numerical solution of ODE boundary value problems, Online software support. <http://www.maplesoft.com/support/help/Maple/view.aspx?path=dsolve/numeric/BVP>.
Nayfeh, A.H., Abdel-Rahman, E.M., Younis, M.I., 2003. A reduced-order model for electrically actuated microbeam-based MEMS. Journal of Microelectromechanical Systems 12, 672–680.
Ouakad, H.M., Younis, M.I., 2010. The dynamic behavior of MEMS arch resonators actuated electrically. International Journal of Non-Linear Mechanics 45, 704–713.
Pane, I.Z., Asano, T., 2008. Investigation on bistability and fabrication of bistable prestressed curved beam. Japanese Journal of Applied Physics 47, 5291–5296.
Park, S., Hah, D., 2008. Pre-shaped buckled-beam actuators: theory and experiments. Sensors and Actuators A: Physical 148, 186–192.
Pelesko, J., Bernstein, D., McCuan, J., 2003. Symmetry and symmetry breaking in electrostatic MEMS. In: Proceedings of Modeling and Simulation of Microsystems, San Francisco, CA, USA, pp. 304–307.
Plaut, R.H., 2009. Snap-through of shallow elastic arches under end moments. Journal of Applied Mechanics 76, 014504-1–014504-3.
Plaut, R.H., Virgin, L.N., 2009. Vibration and snap-through of bent elastica strips subjected to end rotations. Journal of Applied Mechanics 76, 041011-1–041011-7.
Qiu, J., Lang, J., Slocum, A.H., 2004. A curved-beam bistable mechanism. Journal of Microelectromechanical Systems 13, 137–146.
Rhoads, J.F., Shaw, S.W., Turner, K.L., 2008. Nonlinear dynamics and its applications in micro- and nanoresonators. In: Proceedings of DSCC2008 2008 ASME Dynamic Systems and Control Conference, October 20–22, 2008, Ann Arbor, Michigan, USA, Paper DSCC2008-2406.
Saif, M.T.A., 2000. On a tunable bistable MEMS-theory and experiment. Journal of Microelectromechanical Systems 9, 157–170.
Seyranian, A.P., Elishakoff, I., 1989. Modern Problems of Structural Stability. Springer, Vienna, New York.
Shampine, L.F., Reichelt, M.W., Kierzenka, J., 2011. Solving boundary value problems for ordinary differential equations in MATLAB with bvp4c. <http://www.mathworks.com/bvp_tutorial>.
Simitses, G.J., 1989. Dynamic Stability of Suddenly Loaded Sturctures. Springer-Verlag, New York.
Simitses, G.J., Hodges, D.H., 2006. Fundamentals of Structural Stability. Butterworth–Heinemann.
Southworth, D.R., Bellan, L.M., Linzon, Y., Craighead, H.G., Parpia, J.M., 2010. Stress-based vapor sensing using resonant microbridges. Applied Physics Letters 96 (article number 163503).
Thompson, J., Hunt, G., 1973. A General Theory of Elastic Stability. Wiley-Interscience publication, J. Wiley.
Timoshenko, S., 1961. Theory of Elastic Stability. McGraw-Hill, New York.
Villagio, P., 1997. Mathematical Models for Elastic Structures. Cambridge University Press, Cambridge.
Zhang, Y., Wang, Yisongand Li, Z., Huang, Y., Li, D., 2007. Snap-through and pull-in instabilities of an arch-shaped beam under an electrostatic loading. Journal of Microelectromechanical Systems 16, 684–693.